

Natural Kermes Dye as an Effective Additive for Electrochemical Deposition of Nickel from Watts-type Nickel Bath

Manal A. El Sayed¹ and Magdy A.M. Ibrahim^{2,*}

¹ Department of Physics, Faculty of Science and Arts, Qassim University, Bukairiayh, Qassim 51941, KSA

² Department of Chemistry, Faculty of Science, Ain Shams University, Abbassia, Cairo 11566, Egypt

*E-mail: imagdy1963@hotmail.com

Received: 28 January 2019 / Accepted: 23 March 2019 / Published: 10 May 2019

In this work, considerable improvements in the corrosion resistance as well as on the microhardness of the electrodeposited nickel from Watts-type nickel bath has been achieved by using Natural Kermes Dye (NKD) as an effective additive. The investigation was carried out to study the influence of different concentrations of NKD on the polarization behavior, anodic linear stripping voltammetry, cyclic voltammetry, cathodic current efficiency, current-time transients as well as on the microhardness. The microhardness was improved considerably, it changes from 130.4 to 225 kg f mm⁻² in the presence 8.0 x 10⁻⁶ M NKD. Moreover, the corrosion resistance of Ni coating was enhanced about five times in the existence of 1.0 x 10⁻⁵ M NKD. On the other side, the inclusion of NKD to the plating electrolyte leads to a large move in the polarization as well as on the deposition potential to nobler potentials, pointing out a catalytic action of NKD on nickel deposition process. The kinetic information emphasized that the exchange current is significantly increased with enhancing NKD concentration while α_c remains nearly constant, supposes that the addition of NKD does not change the Ni deposition mechanism. The phases and morphology of the nickel coatings were checked in the absence and presence of NKD by XRD and SEM.

Keywords: Natural kermes dye; Ni electrodeposition; corrosion resistance; current efficiency; microhardness.

1. INTRODUCTION

In reverse to chromium which generally exhibits cracks, nickel is comparatively strong metal with excellent ductility [1]. The technology of nickel electroplating has been widely developed to produce various industrial coatings for decorative and functional purposes [2]. This extensive use reviews the beneficial features of nickel as a coating. Most nickel baths, especially those used for decorative purpose, are consists of ‘Watts’ formulation. It is well known that the structural and

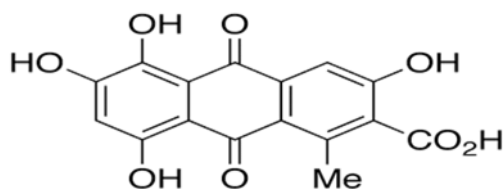
mechanical properties are strongly controlled by the operating conditions, such as composition, temperature, pH, agitation, the presence of additives, and current density. In practice, among these factors, one of the most effective factors in controlling the quality and properties of the nickel deposits, is the use of additives. The additives could be organic and certain metallic compounds chosen to bright and level the metal coatings.

However, a survey of the literature shows a deficiency in research dealing with addition agents for nickel deposition. The addition agents recorded for Watts bath are *cis*-2-butene-1,4-diol and 2-butyne-1,4-diol [3] saccharin [4], L-proline [5] and *p*-ethoxycyanothioformanilide (PECTF) [6]. Moreover, the influence of some amino acids on the electro-kinetics of Ni electrodeposition was studied by several authors [7-10]. Recently, phytic acid is demonstrated as an additive in the Watts bath by Zhang et al. [11]. To our knowledge, no studies have been conducted depending on NKD in electrodeposition processes. Therefore, the present research goals to study the nickel deposition from a Watts-type nickel bath containing NKD to improve the nickel coatings characteristics such as the corrosion resistance as well as the microhardness. In addition, the investigation focusses on the kinetics of nickel plating.

2. EXPERIMENTAL

The electroplating of Ni was carried out galvanostatically applying a Watts-type nickel formulation contains 0.63 M nickel sulfate, 0.09 M nickel chloride, and 0.3 M boric acid in the existence and absence of NKD at pH 3.8 and 25°C.

NKD is a very bright red dye which is produced from the shell of the female insects' clusters on the wood. The advantage of using NKD is not only its color stability, it's easy solubility in water at room temperature but also its cheapness. Its uses have been reported in old Egypt when this color was known as the King's red and used as a painter's pigment. Recently, NKD has been applied as an efficient anticorrosion material for mild steel in an acidic medium [12]. The molecular structure of the NKD is shown in Scheme 1.



Scheme 1. The chemical structure of the natural kermes dye

Solutions used were newly made using analytical reagent class chemicals and distilled water. Steel and Pt plates of the same dimensions (2.4 x 2.5 cm) were applied as cathode and anode severally for nickel plating. A Plexiglass trough (9.0x3.0 cm) has been used as a deposition cell. The steel substrate was mechanically polished with fine emery paper, washed, dehydrated and weighed. A direct current supplier model: GPS-3030DD was applied as a D.C. source. The determination of the cathodic current

efficiency (F%) of nickel deposition was carried out with a Cu coulometer and the equation ($F = W_{\text{Prac}} / W_{\text{theo}}$), where W_{Prac} is the practical weight of the deposit, and W_{theo} is the theoretical weight of the deposit according to Faraday's law [13]. The plating was done for 600 s at 25°C. The throwing power, TP%, was estimated from Field's principle [13].

Meanwhile, the thickness can be calculated from the following equation [2]:

$$X = 12.294 It / A \quad (1)$$

Where X is the thickness (μm) and A is the area being electrodeposited (dm^2), I is the current in amperes and t is the time in hours.

The cathodic polarization was done using steel sheets by moving the potential towards the negative direction with a scan rate of 10 mVs^{-1} . The reference electrode used in this study was silver/silver chloride electrode. Anodic linear stripping voltammetry (ALSV) method was measured using a steel plate as a working electrode, Ag/AgCl reference electrode and a platinum wire as an auxiliary electrode. The deposition of nickel was carried out potentiostatically for a definite time. Then, stripping was done promptly in the same solution by moving the potential towards a more positive direction at a scan rate of 10 mVs^{-1} . Three-electrode cell was used for the cyclic voltammetry measurements. The working electrode was a platinum electrode of exposed area = 0.1963 cm^2 . The Pt electrode was polished before each experiment with a diamond paste until a shiny surface finishing was achieved, then washed with distilled water. The counter-electrode was a platinum net.

The chronoamperometric response was carried out at a platinum disc electrode (0.1963 cm^2). The electrochemical station used was 1000 Gamry Instrument Potentiostat/Galvanostat/ZRA. Scanning electron microscopy model JEOL JEM-1200EX was used to investigate the nickel surface morphology. The microstructure of the nickel coatings was examined by a Shimadzu XRD-6000 diffractometer (40 kV, 30 mA), Ni filter and CuK_α radiation. The microhardness of the nickel deposit was measured using a micro-Vickers hardness tester model HWDM-7. A Knoop indenter was used with a load of 500 g. For the hardness measurements, samples were electroplated for 1 hour to obtain a high thickness (30-32 μm) to prevent the interference with the substrate. Five readings were taken for each sample and an average value was estimated as a microhardness value.

3. RESULTS AND DISCUSSION

3.1. Polarization behavior and Tafel kinetics

Fig .1 clarifies the E/i curve during the electrodeposition of nickel on steel substrate from Watts formulation in the existence and absence of different concentrations of NKD. The introduction of NKD to the Watts bath shifted significantly the polarization curve as well as the deposition potential to nobler potential values i.e. depolarization of the cathode occurs. This behavior could be assigned to the formation of a complex between Ni^{2+} ions and NKD molecule or its reduction product. It appears that the complex formed accelerates the reduction of Ni^{2+} ions on the cathode surface. This point out also that NKD has a catalytic effect for Ni^{2+} reduction at the steel surface and does not act by blocking the active sites on the electrode surface. An identical effect was reported during the deposition of Ni from Watts formulation using L-Proline as an additive [5]. Moreover, Han [14] have concluded that part of

Ni^{2+} ions can form a complex with the electro-reduced product of thiourea, which favored the Ni^{2+} reduction, thereby, giving rise to the depolarization effect.

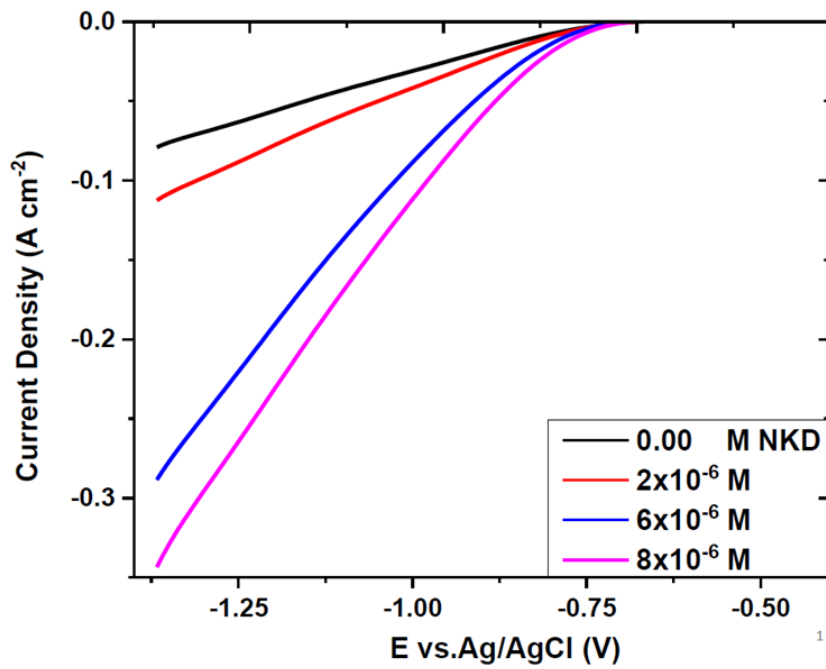


Figure 1. Polarization behavior during nickel deposition on steel substrate from Watts bath in the absence and presence of different concentrations of NKD at pH 3.8 and at 25°C.

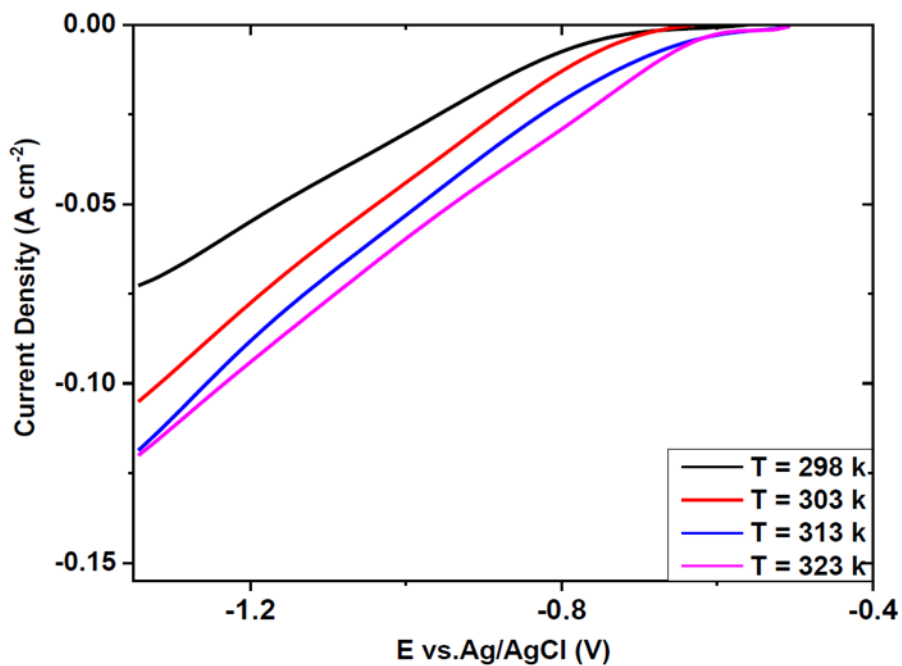


Figure 2. Polarization behavior during nickel deposition on steel substrate from Watts bath at different bath temperatures at pH 3.8.

On the other hand, Fig. 2 displays the influence of elevated temperature on polarization behavior. It is found that the cathodic polarization is shifted towards nobler potentials with enhancing the temperature. This means, rising the bath temperature has a depolarizing effect as a result of its impact on the activation overpotential of reducible ions [15]. In addition, elevation of temperature intensifies the concentration of the reducible species in the diffusion layer as a result of increasing the rate of diffusion. It appears that an increase in temperature declines the stability constant of the complex species and enhances the entity of relatively higher concentrations of the free Ni^{2+} ions [16].

However, Fig. 3 reveals the impact of pH (1.5 - 3.9) on the polarization behavior, the pH of each bath was fixed by add H_2SO_4 or NaOH solution. The cathodic polarization increases as the pH increases. This trend may be related to an increase in hydrogen overpotential.

Kinetic analysis of Ni deposited in the existence and absence of NKD was considered by using Tafel lines which were used to calculate the kinetic variables such as the Tafel slope, β_c , and transfer coefficient α_c (Table 1). The data reveals that as the concentration of NKD is increased, the exchange current, i_0 is appreciably increased. It is established that the exchange current density i_0 is enhanced when the process is activated [17]. On other words, NKD activates the rate of Ni^{2+} ion transfer through the electric double layer.

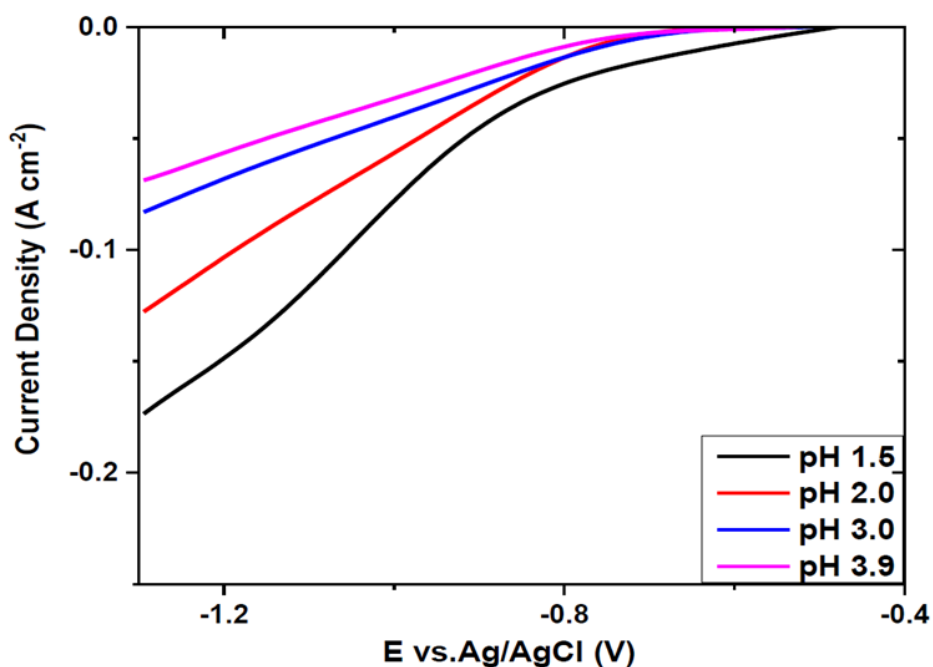


Figure 3. Polarization behavior during nickel deposition on steel substrate from Watts bath at different pH values at 25°C.

The acceleration impact of NKD might be assigned to its complex formation with Ni^{2+} ions, which accelerates the reduction of Ni^{2+} ions. It is observed also that Tafel slopes are lower in a solution containing NKD. In addition, the Tafel slope decreases with raising pH. At the same time, i_0 noticeably decreases whilst α_c is nearly unchanged. Furthermore, elevation of temperature leads to an increase in Tafel slope as well as in i_0 . The values of α_c are comparatively invariant in all cases studied and almost

constant. This reviews that the mechanism of nickel deposition under such conditions is unchanged in the presence of NKD.

3.2. Anodic linear stripping Voltammetry (ALSV)

ALSV was carried out by potentiostatic deposition of Ni on steel at -0.9 V for 100 s. Thereafter, the potential was moved to the positive potential direction and the stripping voltammogram was traced without removing the electrode from the solution. Fig. 4 displays the effect of inclusion of various concentrations of NKD to the electrolyte on the ALSV.

Table 1. Tafel kinetic parameters obtained for different plating solutions

	Exchange current density i_o ($\mu\text{A cm}^{-2}$)	Tafel slopes $-\beta_c$ (V decade $^{-1}$)	Transfer Coefficient α_c
[NKD] / M			
0.00	0.01399	0.915	0.012
2×10^{-6}	0.01545	0.814	0.013
6×10^{-6}	0.03221	0.788	0.013
8×10^{-6}	0.03758	0.762	0.013
pH			
3.8	0.01399	0.915	0.012
3.0	0.02506	0.995	0.012
2.0	0.03622	0.998	0.012
1.5	0.04943	1.000	0.012
Temp./ $^{\circ}\text{C}$			
25	0.01399	0.915	0.012
30	0.02188	1.102	0.011
40	0.02710	1.150	0.011
50	0.03047	1.140	0.012

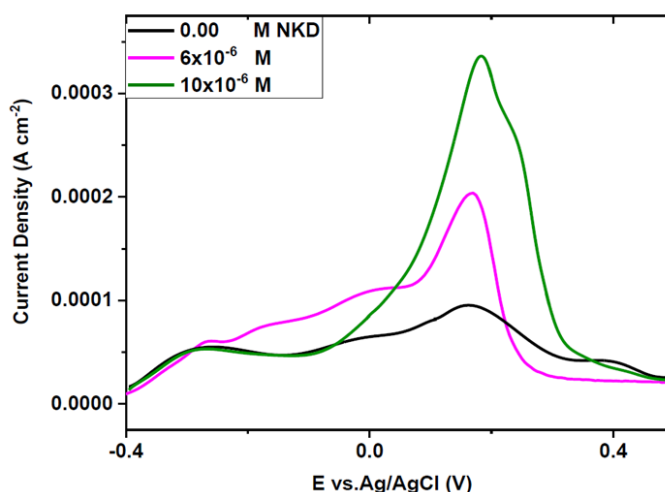


Figure 4. Anodic linear stripping voltammetric curves recorded at steel electrode in the absence and presence of different concentrations of NKD at pH 3.8 and at 25°C.

Not only the intensity of the stripping peak but also the area under the peak increases with increasing the concentration of NKD. This finding is in consistency with the polarization curves in Fig. 1. The voltammograms have only one main oxidation peak (Fig. 4), resulted from the dissolution of Ni deposited formerly. Visual investigation of the steel surface beyond the stripping peak doesn't show any Ni or NiO residual. Consequently, the charge used through anodic stripping could be accepted as an estimation of the amount of nickel deposited, i.e., the area under the peak is a detector for nickel deposited.

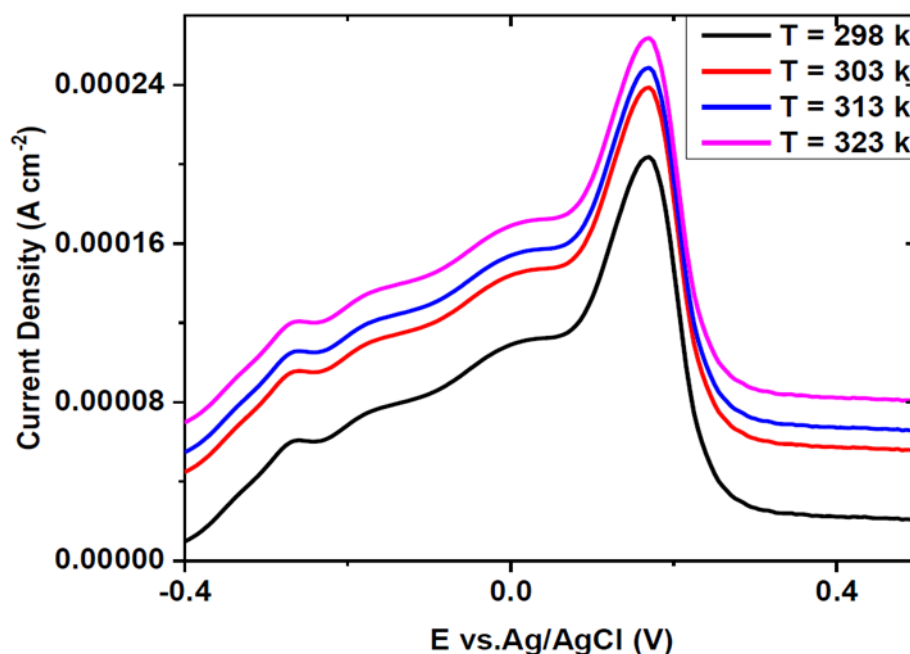


Figure 5. Anodic linear stripping voltammetric curves recorded at steel electrode at different bath temperatures (pH 3.8).

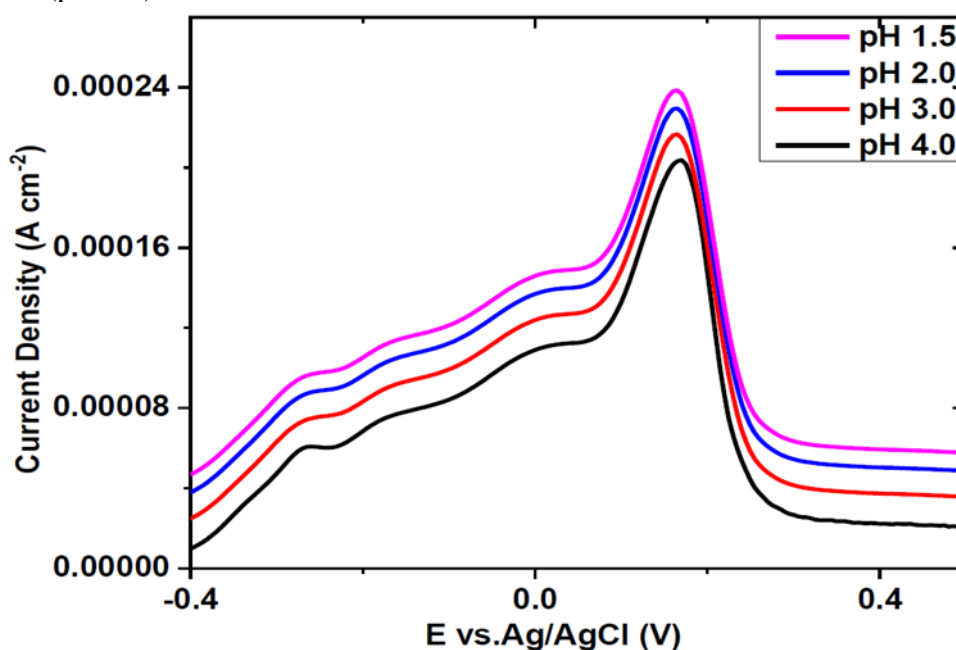


Figure 6. Anodic linear stripping voltammetric curves recorded at steel electrode at different pH and at 25°C.

Fig.5 shows the effect of raising the bath temperature on the ALSV in the presence of NKD. The data reveals also that not only the intensity of the peak increases but also the area under the peak, in agreement with the result shown in Fig.2. This may be explained by the idea that an elevation of solution temperature declines the stability constant of the complex formed between the kermes dye molecule and the Ni^{2+} ions, causing higher concentrations of the free Ni^{2+} ions.

Furthermore, Fig.6 illustrates the impact of pH on ALSV and the results illustrate that the stripping charge for nickel deposition declines with rising pH. This finding also agrees well with the result obtained from the polarization behavior in Fig .3.

3.3. Cathodic current efficiency and throwing power

The effect of NKD concentrations on the F% of nickel electrodeposited was carried out and the results reveal no significant effect on the F% by the addition of NKD to the plating bath (Table 2). It is well established that addition agents on Ni electroplating baths usually has no significant effect or a slight decreasing effect on F% [18]. Li et al. [19] recorded that a minor change of 1~2% in current efficiency is observed when saccharin concentrations ranging from 0.0 to 1.2 g/l was added to nickel sulfate electrolyte.

Table 2. The effect of NKD concentrations on the F% (time 10 min, $i = 2.61 \text{ A/ dm}^{-2}$, 25°C)

[NKD] / M	F%
0.0	98.1
2.0×10^{-6}	98.0
4.0×10^{-6}	97.8
6.0×10^{-6}	97.9
8.0×10^{-6}	98.2
1.0×10^{-5}	98.0
1.2×10^{-5}	97.5
2.0×10^{-5}	97.0

Table 3. The effect of current density and temperature on the F% of nickel deposition in the presence of $6.0 \times 10^{-6} \text{ M NKD}$.

Current density, A dm^{-2}	Thickness/ μm	F%	Temp./ $^\circ\text{C}$	F%
0.17	0.354	88.9	25	98.1
0.87	1.774	98.7	30	97.8
1.22	2.484	98.4	35	95.0
1.74	3.549	98.1	40	89.8
2.61	5.323	98.2	50	85.0
3.48	7.098	98.0	60	82.0

It was found that the NKD concentration of 6.0×10^{-6} M produces shine and smooth deposit and consequently, it is taken as an optimum concentration in all baths used after that. Therefore, the effect of some plating conditions such as current density and bath temperature on the F% was studied at constant plating time 10 min and at a temperature of 25°C in the existence of 6.0×10^{-6} M NKD (Table 3). The average thickness of the nickel coatings at different current densities was recorded in Table 3. Investigation of the results in Table 3 illustrate that increasing the current density has no significant effect on F% and the values were around 98%. Only at very low current, the F% was 88.9% because this very low current is not enough for complete nickel deposition.

The impact of solution temperature (25-60°C) on the F% of nickel plating was carried out from Watts bath in the existence of 6.0×10^{-6} M NKD and the results explore that increasing the bath temperature from 25°C to 60°C decreases the F% from 98.1 to 82% (Table 3). This decreasing effect could be due to the increase in H₂ evolution with increasing the temperature. General speaking, the deposition of Ni²⁺ ions are associated with the discharge of H⁺ ions from water. This decreases the F of nickel deposition (from 100% to 92 - 98%) according to the type of the electrolytic bath.

It is worthwhile to mention here that the measurements of the throwing power of Watts-type nickel formulation in the presence and absence of NKD do not show any significant change (within ± 2%) (data are not included). This means that the inclusion of NKD to the Watts formulation has no remarkable impact on the throwing power.

3.4. Cyclic voltammetry

Fig. 7 displays the cyclic voltammograms of Ni electrodeposition in the presence of different NKD concentrations on Pt electrode. It was observed that there is no difference in the oxidation peak of the cyclic voltammogram for the anodic peak and it is planned to follow up the variation in reduction peak only. It is found that the reduction potential is moved to nobler potentials in the presence of NKD. This action of NKD could be assigned to its complex formation with Ni²⁺ ions, as previously mentioned, indicating that the complex formed accelerates the reduction of Ni²⁺ ions. This reveals that NKD doing as an activator for nickel deposition on the steel and does not act by blocking the surface-active centers for nickel deposition. This data is in good agreement with the data in Fig. 1.

3.5. Chronoamperometry

Chronoamperometric investigation (current–time transient) was accomplished to analyze the nucleation and growth mechanism of nickel deposition. A representative potentiostatic *i*–*t* transients recorded in the course of Ni²⁺ ions reduction in the absence and presence of various concentrations of NKD at a deposition potential of –0.9 V is displayed in Fig. 8. It is observed that the current enhances rapidly to a maximum value and then decreases slightly to attain steady state current.

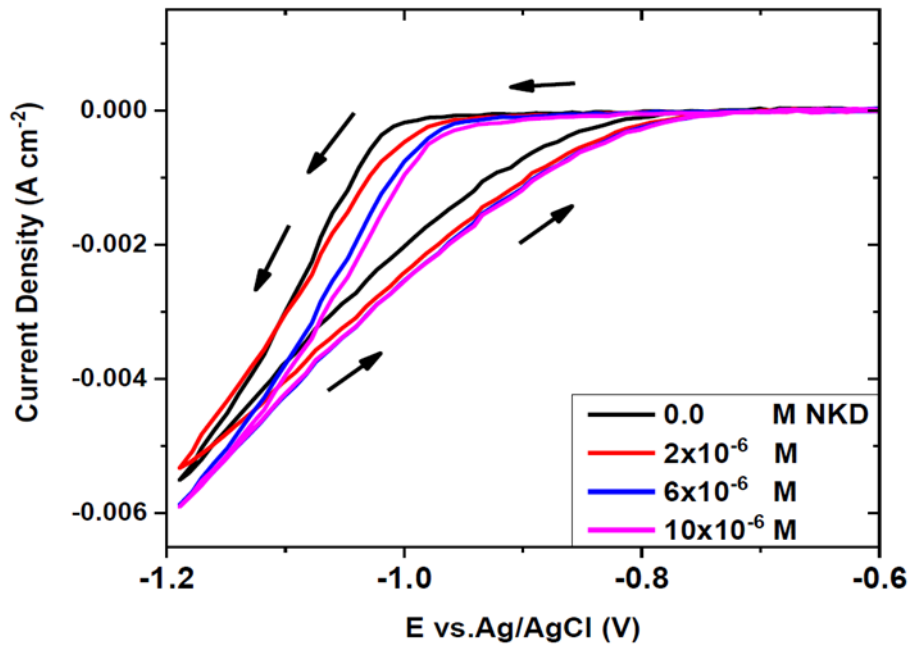


Figure 7. Cyclic voltammetric curves recorded at Pt disc electrode in the absence and presence of different concentrations of NKD at pH 3.8 and at 25°C (scan rate = 10 mVs^{-1}).

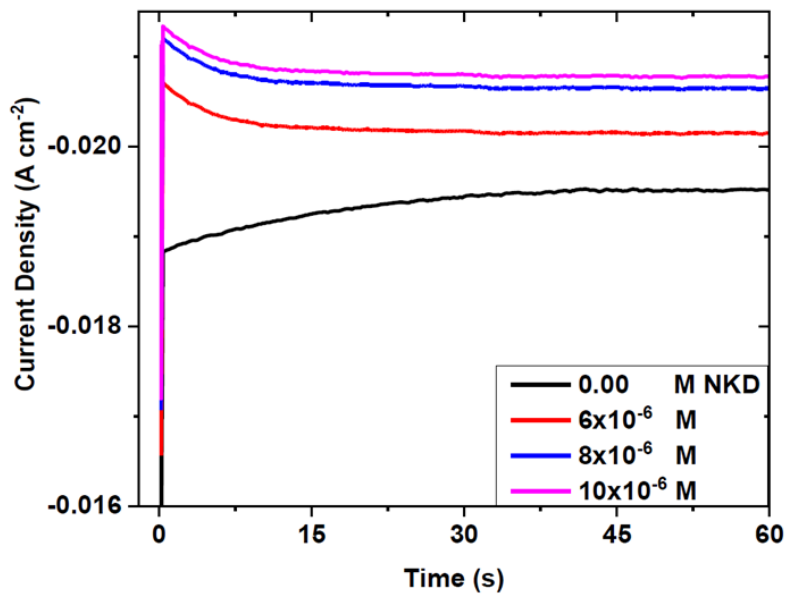


Figure 8. Potentiostatic current – time transient for nickel deposition from Watts bath recorded at Pt disc electrode in the absence and presence of different concentrations of NKD at a deposition potential of -0.9 V.

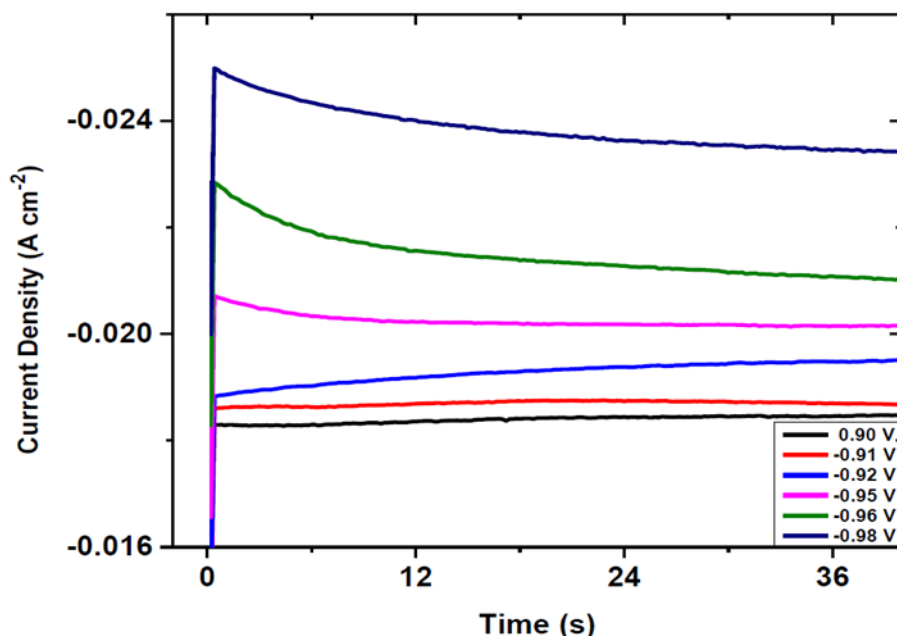


Figure 9. Potentiostatic current – time transient for nickel deposition from Watts bath recorded at Pt disc electrode in the presence of NKD at different deposition potential.

These transients are typical of the nucleation and phase growth of metal on the electrode surface. Moreover, the data suggest that nucleation growth is not a diffusion-controlled process. In the beginning, the current increases sharply as the electroactive area increases either as each independent nucleus grow in size (instantaneous growth) and/or the number of nuclei increases (progressive growth). The current transients achieved steady state when the uncovered surface becomes totally saturated [20]. The small variation of the steady state current with time suggests that after overlapping of the growth nuclei and development of a continuous layer, thickening occurs. On the other hand, a series of transients were carried out at different deposition potentials as shown in Fig. 9. The steady state current is, increases and the time scale of the transient decrease as the deposition potential is made more negative.

3.6. Corrosion behavior

3.6.1. Anodic potentiodynamic method

The corrosion behavior of nickel coatings prepared from Watts formulation in the absence and presence of NKD was investigated in aggressive chloride ions environment using anodic polarization method (Fig. 10). The potential was scanned towards nobler potentials. Nickel deposits examined exhibited an active-passive-transpassive tendency. The corrosion current (i_{corr}), the corrosion rate in mpy, corrosion potential (E_{corr}), and the cathodic and anodic Tafel slopes were evaluated, and the data are tabulated in Table 4. It is found that the i_{corr} is significant decreases and E_{corr} is proceeded to nobler potential direction, in the status of coatings achieved from Watts formulation containing NKD. This indicates that the nickel coatings prepared in the presence of NKD have a higher corrosion resistance relative to nickel coating achieved without NKD. On the other hand, both the anodic and cathodic Tafel slopes were decreased in the presence of NKD.

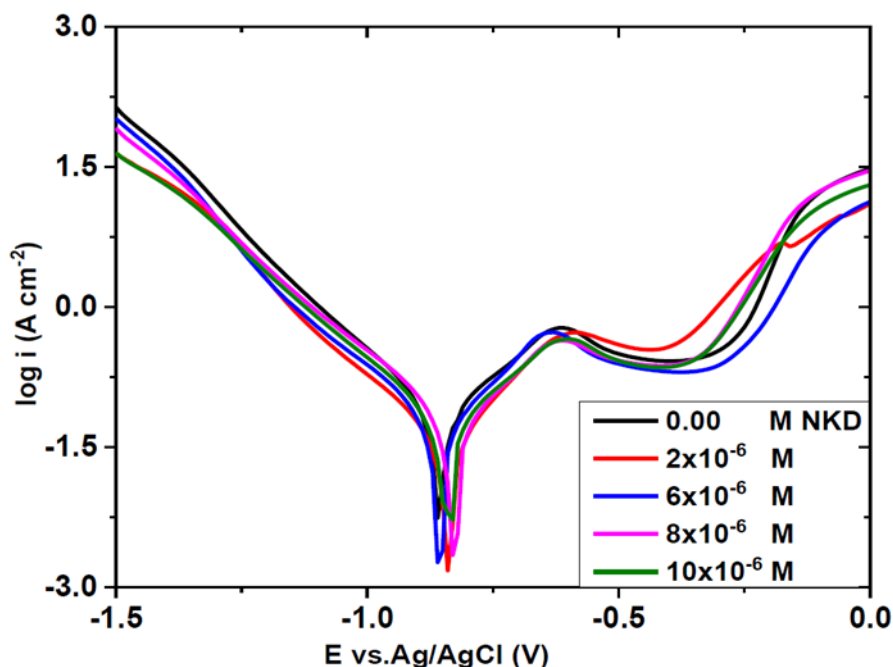


Figure 10. Anodic potentiodynamic curves for nickel coating deposited on steel in the absence and presence of different NKD concentrations in 3.5% NaCl.

Table 4. Electrochemical corrosion parameters of Ni coatings deposited at different NKD concentrations.

NKD / M	$i_{corr} / \mu A cm^{-2}$	Corr. Rate / mpy	$-E_{corr} / mV$	$\beta_a (V decade^{-1})$	$-\beta_c (V decade^{-1})$
0.00	121.8	63.00	673.7	0.601	0.527
2×10^{-6}	71.2	36.80	728.0	0.362	0.265
6×10^{-6}	67.6	34.96	728.0	0.348	0.263
8×10^{-6}	37.6	19.47	704.5	0.299	0.310
1×10^{-5}	21.3	10.95	701.5	0.250	0.252

3.6.2. Open circuit potential (OCP)

Fig. 11 clarifies the relation between the free corrosion potential for nickel coating deposited at $2.61 A dm^{-2}$, pH 3.8, and at $25^{\circ}C$ for 600 s in the existence and absence of NKD in aggressive chloride ions environment. At the beginning of immersion, the potential for all samples has high values which can be described by the time required for the Cl^{-} ions to arrive by diffusion to the cathode surface. This time is very short in case of the sample prepared without NKD relative to other samples prepared in the presence of NKD (takes longer time). On the other hand, the nickel deposited from Watts bath containing NKD possesses nobler potentials than that formed without NKD, i.e. it has a lower corrosion rate. This data fixed the data earned from anodic polarization (Fig. 10). Samples studied in the presence of NKD showed that the steady-state potential is achieved in about 4 hours while that of the blank it might require much more time to attain a steady state.

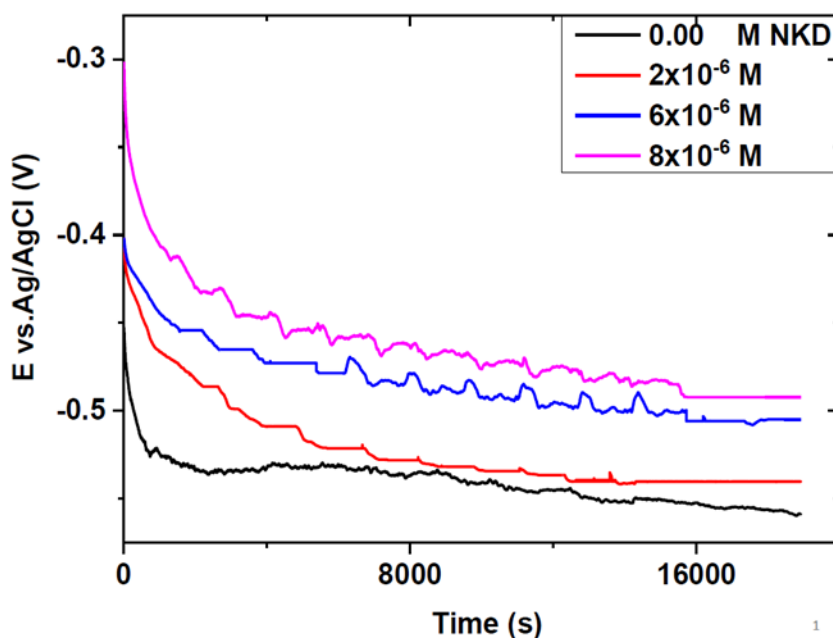


Figure 11. Free corrosion potentials vs. time for nickel coating deposited on steel in the absence and presence of NKD in 3.5% NaCl solution.

3.6.3. Electrochemical impedance spectroscopy (EIS)

The Nyquist profile illustrations of impedance spectra of nickel coatings electrodeposited in the absence and presence of NKD is performed after immersion in 3.5 % NaCl solution for 1.0 hour as demonstrated in Fig. 12. The impedance plot displays depressed semicircles, corresponding to a charge-transfer resistance in parallel with an equivalent capacitance, which can be better expressed in terms of a constant phase element (CPE). The data reveal that as NKD concentration was increased, the charge transfer resistance R_{ct} values decreased. From the EIS Nyquist profile, each EIS plot consists of two capacitive loops above the real axis. At high frequency, the capacitive loop may be stimulated by the electrodeposited nickel coating, while at low-frequency, the capacitive loop is associated with the corrosion charge transfer resistance. The R_{ct} can disclose the rate of corrosion. The lower the value of R_{ct} , the larger the value of the corrosion rate. It is recorded that the R_{ct} of nickel coating (blank) ($R_{ct} = 332.6 \Omega$) is much lower than those of the coating prepared in the presence of NKD ($R_{ct} = 408.6 \Omega$ for $2.0 \times 10^{-6} \text{ M}$ NKD and $R_{ct} = 435.3 \Omega$ for $6.0 \times 10^{-6} \text{ M}$ NKD), which means the corrosion rate of the blank coating is higher, and the coatings prepared in the presence of NKD possesses good corrosion resistance. This data is in accordance with the data noticed from the anodic potentiodynamic and the open circuit potential method.

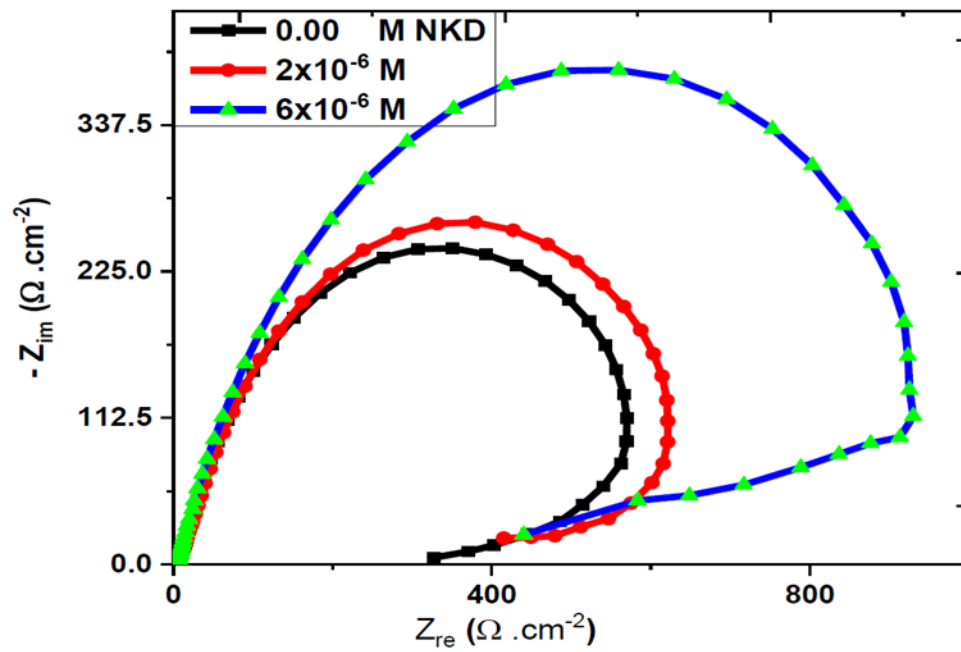


Figure 12. Nyquist plot for nickel coating deposited on steel in the absence and presence of different concentrations of NKD in 3.5% NaCl.

3.7. Surface morphology and XRD

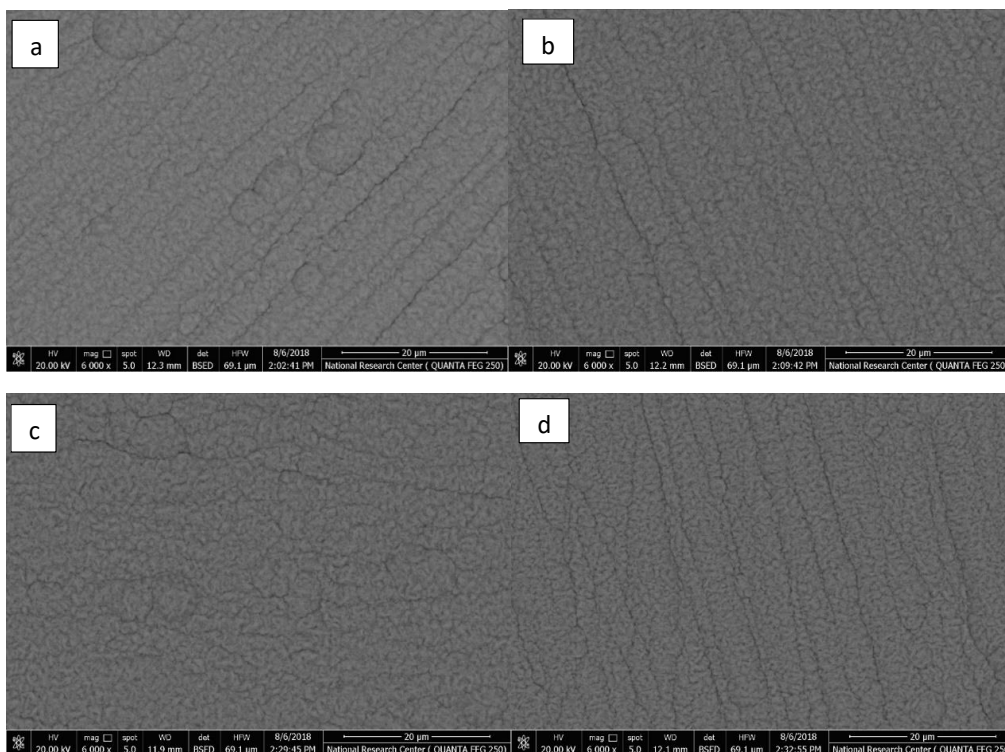


Figure 13. Photomicrographs of nickel deposited on steel in the absence and presence of different concentrations of NKD, pH 3.8, t = 10 min and at 25°C (a: 0.0 M); (b: 6 x 10⁻⁶ M); (c: 8 x 10⁻⁶ M); and (d: 1.2 x 10⁻⁵ M).

The surface morphology of the nickel coatings in the existence and absence of NKD was investigated by scanning electron microscope and the photomicrographs are shown in Fig. 13. The nickel deposits are formed in elongated arrangements having very close and packed structure. In the absence of NKD (Fig. 13a) the deposit contains large agglomeration in a circular shape. However, in the presence of NKD the grains become finer and still deposited in an elongated manner but without such circular agglomeration (Fig. 13 b-d). The plated surface is free of imperfections e.g. abscess, cruelty, pits, cracks, discoloration, stains, and un-plated zones.

On the other hand, the microstructure of the nickel coatings prepared from Watts formulation in the existence and absence of NKD was investigated by X-ray diffraction (Fig. 14). The data point out that the nickel deposited in the presence and absence of NKD exhibited a face-centered cubic structure, with a very intense (111) peak (preferred orientation) i.e. nickel crystallites were oriented parallel to (111) plane. This crystallographic orientation is in conformity with that typically observed for these deposits [21]. As a conclusion, the inclusion of NKD did not alter the crystallographic orientation of the crystal planes of the electrodeposited nickel.

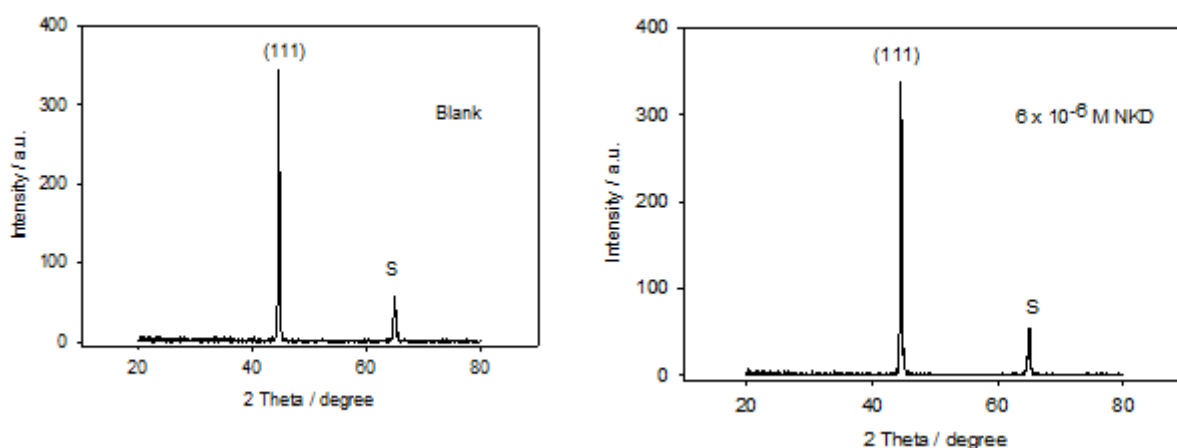


Figure 14. XRD patterns of nickel coatings deposited on steel (at pH 3.8, $t = 10$ min and at 25°C) in the absence and presence of NKD, S is the steel substrate.

3.8. Microhardness of nickel coatings

The Vickers microhardness of some as-deposited nickel from Watts bath ($i = 2.61 \text{ Adm}^{-2}$, 25°C , $t = 60$ min, and thickness range from $30\text{-}32 \mu\text{m}$) was compared with that resulted from baths containing NKD (Table 5). The results show that the microhardness of nickel coatings prepared from baths containing NKD is greater than that of nickel deposited from Watts bath without NKD. It was found that the microhardness increases from 130.4 in the absence of NKD to $225.2 \text{ kg f mm}^{-2}$ in the presence of $1.2 \times 10^{-5} \text{ M NKD}$. The possible reason may be due to the increased incorporation of the organic dye material into the coating, as found by Huang [22]. He noticed that the increased presence of ammonium and sulfate ions produced harder and higher stressed nickel coatings from sulphamate baths. On the other hand, sample measured at a high current density ($i = 4.35 \text{ A dm}^{-2}$) shows a slight decrease in hardness, may be due to the formation of coarse-grained deposits at such high current (Table 5).

Table 5. The microhardness of nickel deposited on steel at different concentrations of NKD and at a high current density (thickness = 30-32 μm).

[NKD]/ M	Microhardness kg f mm^{-2}
0.00	130.4
6.0×10^{-6}	148.6
8.0×10^{-6}	225.0
1.2×10^{-5}	225.2
6.0×10^{-6}	215.8*

* This sample was deposited using $i = 4.35 \text{ Adm}^{-2}$

4. CONCLUSION

Review of the obtained outcome emerge the following interesting points:

1. The inclusion of NKD to the Watts bath led to considerable improvements in the corrosion resistance as well as on the microhardness of nickel coatings.
2. The inclusion of NKD moved significantly the polarization and the plating potential to more noble potentials, referring to the acceleration action of NKD on the deposition of Ni^{2+} ions.
3. The relatively constant values of α_c suggest that the mechanism of Ni deposition is not altered by the presence of NKD.
4. The inclusion of NKD has no significant impact on the cathodic current efficiency as well as on the throwing power.
5. The presence of NKD did not change the preferential orientation of the of nickel crystal planes as shown by XRD analysis.

ACKNOWLEDGMENT

The authors gratefully acknowledge Qassim University, represented by the Deanship of Scientific Research, on the material support for this research under the number (3482-cosab-2018-1-14-S) during the academic year 1439H/ 2018 AD.

References

1. R.A.F. Hammond, *Some Engineering Aspects of Electrodeposition, Products Finishing*, 79 (10) (2015) 9.
2. I. Rose and C. Whittington, *Nickel Plating Handbook*, Nickel Institute, Brussels, Belgium, 2014.
3. E. P. S. Schmitz, S. P. Quinaia, J. R. Garcia, C. K. de Andrade and M. C. Lopes, *Int. J. Electrochem. Sci.*, 11 (2016) 983.
4. T. Osaka, T. Sawaguchi, F. Mizutani, T. Yokoshima, M. Takai, and Y. Okinaka, *J. Electrochem. Soc.*, 146 (9) (1999) 3295.
5. N.F. El Boraie and M.A.M. Ibrahim, *Surf. Coat. Technol.*, 347 (2018) 113.
6. M. A. M. Ibrahim and S.N. Alamri, *J. Appl. Surf. Finish.*, 2 (4), (2007) 332.

7. M. Ebadi, J.B. WAN, Y. Sim and M.R. Mahmoudian, *Metall. Mater. Trans. A* 44 (11) (2013) 5096.
8. Y. Zhang and B. Pan, *J. Electroanal. Chem.*, 796 (2017) 43.
9. N.V. Sotskaya, L.V. Saprionova, O.V. Dolgikh, *Prot. Met. Phys. Chem. Surf.*, 50 (1) (2014) 22.
10. N.V. Sotskaya, L.V. Saprionova, O.V. Dolgikh, *Russ. J. Electrochem.* 50 (12) (2014) 1137.
11. C. Zhang, H. Liu, P. Ju, L. Zhu and W. Li, *J. Electrochem. Soc.*, 165 (11) D518-D525 (2018).
12. N. F. El Boraie, S. Abdel Halim, and M. A.M. Ibrahim, *Anti-Corrosion Methods and Materials*, 65 (6) (2018) 626.
13. M. A. M. Ibrahim, *J. Chem. Technol. Biotechnol.*, 75 (2000)745.
14. Q. Han, K. Liu, J. Chen, and X. Wei, *Int. J. Hydrogen Energy*, 28 (2003) 1207.
15. V. B. Singh and P. K. Tikoo, *Electrochim. Acta*, 22 (1977) 1201.
16. S.S. Abd El Rehim, M.A.M. Ibrahim and M.M. Dankeria, *J. Appl. Electrochem.*, 32(2002) 1019.
17. K. R. Marikkannu & G. P. Kalaignan, *J. Appl. Surf. Finish.*, 1 (4), (2006) 282.
18. B.C. Tripathy, P. Singh, D.M. Muir, and S.C. Das, *J. Appl. Electrochem.*, 31 (3) (2001) 301.
19. Y. Li, J. Yao, and X. Huang, *Int. J. Metall. Mater. Eng.*, 2(2016)123.
20. E. A. Abd El Maguid, S.S. Abd El Rehim, and E.M. Mostafa, *Trans. IMF*, 77 (1999) 188.
21. M. A. M. Ibrahim and R. M. Al Radadi, *Int. J. Electrochem. Sci.*, 10 (2015) 4946.
22. C. Huang, *Plat. & Surf. Finish.* 81 (1994) 64.

© 2019 The Authors. Published by ESG (www.electrochemsci.org). This article is an open access article distributed under the terms and conditions of the Creative Commons Attribution license (<http://creativecommons.org/licenses/by/4.0/>).